Theor Chem Acc (2007) 118:203–210
DOI 10.1007/s00214-007-0271-0

REGULAR ARTICLE

# A computer simulation of model discotic dimers

**Isabella Miglioli · Luca Muccioli · Silvia Orlandi · Matteo Ricci · Roberto Berardi · Claudio Zannoni**

Received: 1 February 2007 / Accepted: 15 February 2007 / Published online: 20 March 2007


**Abstract** We set up a model for discotic liquid crystal dimers and study, by means of Monte Carlo simulations, their phase behaviour and self–assembling properties, in comparison with the simpler monomeric case. Each discotic dimer is described by two oblate Gay–Berne ellipsoids connected by a flexible spacer, modelled by a harmonic "spring" of three different lengths. We find that dimerization in general yields produces a significant change on the phase behaviour, with an increase of the columnar–nematic transition temperature, a widening of the nematic region and the apparent suppression of the crystalline phase in favour of the columnar phase up to very low temperatures. Longer spacers prove to ease the formation of columns and to increase the orientational order.

**Keywords** Monte Carlo · Triphenylenes · Gay–Berne · Columnar phase · Liquid crystals

## 1 Introduction

Disc-shaped molecules, consisting of a flat or nearly flat rigid core surrounded by a variable number of aliphatic chains, organize in a wide variety of mesophases [1–3] with different types of structures, e.g. nematic, columnar and lamellar. However, the vast majority of discotic liquid crystals (DLC) only form columnar phases, probably due to packing and to the synergic effect of the strong $\pi$–$\pi$ interactions of the polyaromatic cores and of the weaker interactions between the aliphatic chains [4]. In the columnar phases the discs are stacked one on top of the other, thus generating columns, i.e., one-dimensional ordered structures [5], whereas the discotic nematic phase features an orientationally ordered arrangement of discs with no long-range translational order.

Among the many mesogenic units used as cores for DLCs, the tris-annulated benzene system "triphenylene" has been the focus of great attention from material scientists, because of its thermal and chemical stability, symmetry, easily tailored chemical synthesis, and finally the ability to organize in a variety of mesophases. The triphenylene-based discotics possess an electron-rich core that makes them suitable for doping with electron acceptors [6], thus becoming organic semiconductors; they have been studied for their peculiar physical properties such as one-dimensional charge [7] and energy transport, electroluminescence, and, last but not least, alignment and self-assembling capabilities into anisotropic structures on surfaces [8].

An important way of creating new families of liquid crystals (LC) with modulated functional properties is that of joining mesogens to yield dimers, oligomers and eventually polymers. Unfortunately, even though the chemistry of selected discotic based dimers, oligomers and polymers has already been examined, the number of reported discotic dimers [9] or liquid crystalline polymers containing disc-like mesogens, either as side groups or within the main chain, is relatively small. Thus, the chemical and physical behaviours of this family of mesogens have not yet been thoroughly investigated, and fully understood [10].

Our aim is to model a discotic dimer system, in order to find out possible variations of the phase diagram and self-assembling properties with respect to the monomeric mesogen. In particular, we intend to verify to which extent, in the presence of dimerization, the discotics still retain their

Contribution to the Fernando Bernardi memorial issue.

I. Miglioli · L. Muccioli · S. Orlandi · M. Ricci · R. Berardi · C. Zannoni (✉)
Dipartimento di Chimica Fisica ed Inorganica and INSTM,
Viale Risorgimento, 4, 40136 Bologna, Italy
e-mail: Claudio.Zannoni@unibo.it

ability to form columnar phases. We shall employ Monte Carlo (MC) computer simulation techniques, already successfully applied to the investigation of calamitic liquid–crystalline dimers [11–14] and polymers [15,16], that offer a tool for establishing a relation between molecular structure and the macroscopic behaviour of mesogens [17]. This approach first entails some assumptions and simplifications about the molecular shape; second it requires the specification and parameterization of a suitable interaction potential.

## 2 Discotic monomer and dimer models

We model discotic monomers as oblate uniaxial ellipsoids interacting with the pairwise attractive–repulsive Gay–Berne (GB) potential (see, e.g. [17–19])

$$U_{\mathrm{GB}} = 4\epsilon_0 \epsilon^{(\mu,\nu)}(\hat{\mathbf{z}}_i, \hat{\mathbf{z}}_j, \hat{\mathbf{r}}_{ij}) \times \left[ \left\{ \frac{\sigma_{ff}}{r - \sigma(\hat{\mathbf{z}}_i, \hat{\mathbf{z}}_j, \hat{\mathbf{r}}_{ij}) + \sigma_{ff}} \right\}^{12} - \left\{ \frac{\sigma_{ff}}{r - \sigma(\hat{\mathbf{z}}_i, \hat{\mathbf{z}}_j, \hat{\mathbf{r}}_{ij}) + \sigma_{ff}} \right\}^{6} \right], \quad (1)$$

where $\mathbf{r}_{ij}$ is the vector joining the centres of discs, $i$ and $j$, and $\hat{\mathbf{z}}_i, \hat{\mathbf{z}}_j$ are unit vectors along their axes (see Fig. 1). The analytical expression for the interaction strength $\epsilon^{(\mu,\nu)}(\hat{\mathbf{u}}_i, \hat{\mathbf{u}}_j, \hat{\mathbf{r}}_{ij})$ and for the range function $\sigma(\hat{\mathbf{u}}_i, \hat{\mathbf{u}}_j, \hat{\mathbf{r}}_{ij})$, in terms of the disc thickness and diameter $\sigma_{ff}$, $\sigma_{ss}$, and well depths $\epsilon_{ff}$, $\epsilon_{ss}$, as well as the parameters $\mu$, and $\nu$ that define the details of the model are introduced in [17,18,20]. Here, instead of the widely diffused parameterization proposed by Emerson et al. [19,21], we employed a more realistic one, specifically derived from a fit of the intermolecular energies and the pair distributions calculated from the trajectories of an atomistic simulation of hexaoctyl thio triphenylene [22], where $\sigma_{ff} = 0.375\ \sigma_0$, $\sigma_{ss} = 1.925\ \sigma_0$, $\epsilon_{ff} = 0.3\ \epsilon_0$, $\epsilon_{ss} = 2.0\ \epsilon_0$, and $\mu = 1$, $\nu = 0$. Here, and in the rest of the paper, we give all the lengths in units and the energies in units of $\sigma_0$ and $\epsilon_0$, roughly corresponding for a triphenylene monomer to 10 Å and 30 kcal/mol.

Considering the dimer model, we notice that most discotic twins have a structure similar to that in Fig. 2, where the two oblate units are connected by a flexible spacer [10], even though some examples of rigid linkers are also known [9]. We thus represent the DLC dimer by two GB oblate discs connected by a spring as in Fig. 1. The discotic monomer is assumed to have a bonding site [15] placed on the disc border, at $(\sigma_{ss}/2, 0, 0)$. The bond cannot break during the simulation (differently from a H-bond driven dimerization process [14]), but we assume that it can to some extent stretch and bend. Thus, besides the GB interaction between a connected pair of monomers as in Eq. 1, a suitable energy contributions involving the separation between two linked bonding sites $r_{ij}^{\mathrm{BND}}$ and

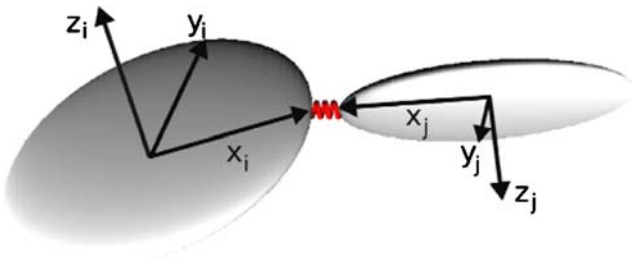


**Fig. 1** Sketch of the discotic dimer model and of the axis system used: as indicated, the bond is along the $x$ direction, and the $z$ axis, used for computing the order parameter, is perpendicular to the monomer disc plane

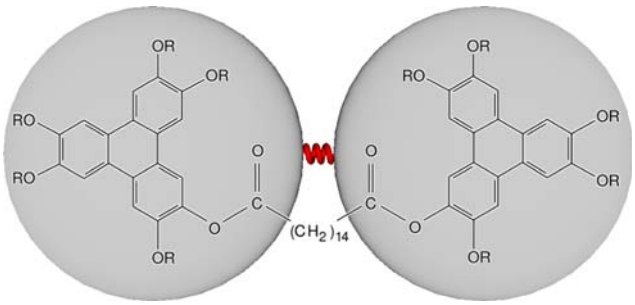


**Fig. 2** Molecular structure of the experimentally characterized discotic dimer DHAT5-C14 ($R = -C_5H_{11}$) [23] superimposed to the *top-view* sketch of a coplanar dimeric model

the bending angle $\theta_{ij}$ (i.e., the angle between molecular axes $\mathbf{x}_i$ and $\mathbf{x}_j$) are added (Eq. 2). For both the effects we assume a harmonic form with specific equilibrium separation $r_d$, and bend angle $\theta_d$ for the dimer:

$$U_{\mathrm{BND}} = \epsilon_0 \sum_{\mathrm{bonds}} \kappa_d (r_{ij}^{\mathrm{BND}} - r_d)^2 + \epsilon_0 \sum_{\mathrm{angles}} \kappa_\theta (\theta_{ij} - \theta_d)^2. \quad (2)$$

In this case, a torsional term was not included as we intend to model an alkyl spacer linking the two discs long enough to allow each one to rotate quite freely, like, e.g., for the dimer DHAT5-C14 [23] (Fig. 2). Therefore, the total energy of the dimer system consists only in the sum of GB plus stretching and bending contributions.

## 3 Monte Carlo simulations

We have performed MC NPT simulations for four different systems: a monomeric one (*M*) and three dimer systems with different spacer lengths (*D0, D1, D2*). The samples consisted of $N = 2,000$ monomer discs (either bonded or not) contained in an orthorhombic box. The reduced pressure in all cases was $P^* = 3$, the cutoff radius $r_c = 2.8\,\sigma_0$, and 3D periodic boundary conditions were used. We run a sequence of computer experiments at different temperatures $T^*$ in steps

**Table 1** Average simulation values for the dimensionless Gay–Berne energy $U^*_{GB}$, elastic energy $U^*_{BND}$, number density $\rho^*$ and for the second rank order parameter $\langle P_2 \rangle$, for dimer models *D0, D1, D2*. Statistical averages are $\pm 0.01$ for all quantities

| $T^*$ | *D0* | | | | *D1* | | | | *D2* | | | |
|---|---|---|---|---|---|---|---|---|---|---|---|---|
| | $\langle U^*_{GB} \rangle$ | $\langle U^*_{BND} \rangle$ | $\langle \rho^* \rangle$ | $\langle P_2 \rangle$ | $\langle U^*_{GB} \rangle$ | $\langle U^*_{BND} \rangle$ | $\langle \rho^* \rangle$ | $\langle P_2 \rangle$ | $\langle U^*_{GB} \rangle$ | $\langle U^*_{BND} \rangle$ | $\langle \rho^* \rangle$ | $\langle P_2 \rangle$ |
| 0.10 | −2.65 | 0.22 | 0.78 | 0.92 | −2.91 | 0.08 | 0.80 | 0.93 | −3.10 | 0.08 | 0.83 | 0.98 |
| 0.15 | −2.57 | 0.28 | 0.77 | 0.92 | −2.81 | 0.12 | 0.79 | 0.93 | −2.99 | 0.12 | 0.81 | 0.95 |
| 0.20 | −2.48 | 0.34 | 0.76 | 0.92 | −2.71 | 0.16 | 0.78 | 0.93 | −2.88 | 0.15 | 0.80 | 0.95 |
| 0.25 | −2.39 | 0.40 | 0.74 | 0.92 | −2.59 | 0.19 | 0.76 | 0.93 | −2.76 | 0.19 | 0.78 | 0.95 |
| 0.30 | −2.29 | 0.46 | 0.73 | 0.92 | −2.49 | 0.23 | 0.74 | 0.93 | −2.64 | 0.23 | 0.77 | 0.94 |
| 0.35 | −2.19 | 0.52 | 0.72 | 0.92 | −2.38 | 0.27 | 0.73 | 0.93 | −2.51 | 0.26 | 0.75 | 0.94 |
| 0.40 | −2.09 | 0.58 | 0.70 | 0.92 | −2.25 | 0.30 | 0.71 | 0.92 | −2.39 | 0.30 | 0.73 | 0.93 |
| 0.50 | −1.89 | 0.70 | 0.68 | 0.91 | −2.05 | 0.38 | 0.68 | 0.92 | −2.16 | 0.37 | 0.69 | 0.93 |
| 0.60 | −1.70 | 0.82 | 0.65 | 0.91 | −1.95 | 0.46 | 0.65 | 0.92 | −1.84 | 0.45 | 0.65 | 0.92 |
| 0.63 | −1.65 | 0.86 | 0.64 | 0.91 | −1.81 | 0.48 | 0.64 | 0.91 | −1.88 | 0.47 | 0.64 | 0.92 |
| 0.67 | −1.12 | 0.90 | 0.59 | 0.88 | −1.79 | 0.51 | 0.63 | 0.92 | −1.80 | 0.50 | 0.63 | 0.92 |
| 0.70 | −1.09 | 0.94 | 0.59 | 0.87 | −1.31 | 0.53 | 0.59 | 0.87 | −1.33 | 0.53 | 0.58 | 0.87 |
| 0.80 | −0.95 | 1.06 | 0.56 | 0.86 | −1.17 | 0.61 | 0.56 | 0.85 | −1.17 | 0.60 | 0.55 | 0.86 |
| 0.90 | −0.85 | 1.18 | 0.53 | 0.85 | −1.07 | 0.69 | 0.53 | 0.84 | −1.07 | 0.68 | 0.53 | 0.83 |
| 1.00 | −0.78 | 1.30 | 0.51 | 0.83 | −0.98 | 0.77 | 0.51 | 0.81 | −0.99 | 0.75 | 0.50 | 0.83 |
| 1.10 | −0.70 | 1.42 | 0.49 | 0.81 | −0.91 | 0.85 | 0.49 | 0.82 | −0.91 | 0.83 | 0.49 | 0.82 |
| 1.20 | −0.64 | 1.54 | 0.47 | 0.79 | −0.85 | 0.93 | 0.47 | 0.79 | −0.86 | 0.90 | 0.46 | 0.78 |
| 1.30 | −0.59 | 1.66 | 0.45 | 0.76 | −0.79 | 1.01 | 0.45 | 0.78 | −0.80 | 0.98 | 0.45 | 0.78 |
| 1.40 | −0.54 | 1.78 | 0.43 | 0.74 | −0.74 | 1.09 | 0.44 | 0.74 | −0.76 | 1.06 | 0.43 | 0.75 |
| 1.50 | −0.50 | 1.90 | 0.42 | 0.71 | −0.70 | 1.17 | 0.42 | 0.72 | −0.72 | 1.13 | 0.41 | 0.72 |
| 1.60 | −0.47 | 2.02 | 0.40 | 0.68 | −0.66 | 1.25 | 0.40 | 0.68 | −0.68 | 1.21 | 0.40 | 0.68 |
| 1.70 | −0.43 | 2.14 | 0.38 | 0.60 | −0.62 | 1.34 | 0.39 | 0.63 | −0.65 | 1.29 | 0.38 | 0.63 |
| 1.80 | −0.40 | 2.25 | 0.36 | 0.33 | −0.59 | 1.42 | 0.37 | 0.56 | −0.62 | 1.36 | 0.37 | 0.55 |
| 1.85 | −0.39 | 2.31 | 0.35 | 0.33 | −0.58 | 1.46 | 0.36 | 0.50 | −0.61 | 1.40 | 0.36 | 0.49 |
| 1.90 | −0.38 | 2.37 | 0.34 | 0.16 | −0.57 | 1.50 | 0.34 | 0.17 | −0.60 | 1.44 | 0.34 | 0.26 |
| 2.00 | −0.34 | 2.49 | 0.33 | 0.15 | −0.53 | 1.59 | 0.33 | 0.10 | −0.57 | 1.52 | 0.33 | 0.13 |
| 2.10 | −0.30 | 2.61 | 0.32 | 0.10 | −0.49 | 1.67 | 0.32 | 0.07 | −0.53 | 1.60 | 0.32 | 0.08 |
| 2.20 | −0.27 | 2.73 | 0.32 | 0.08 | −0.46 | 1.75 | 0.32 | 0.06 | −0.50 | 1.67 | 0.31 | 0.06 |

of 0.1 or less, starting from $T^* = 2.2$ and cooling down to $T^* = 0.1$, a range wide enough not only for both isotropic–nematic and nematic–columnar transitions, but also for the columnar-solid to take place. In this set of simulations, the starting configuration for each dimer system was obtained taking two monomers and binding them with harmonic constant $\kappa_d = 1,000\sigma_0^{-2}$, bond angle $\theta_d = 180°$, bending harmonic constant $\kappa_\theta = 17.5$ rad$^{-2}$; hence, the resulting dimer was replicated 1,000 times. We considered three different bond lengths $r_d$: in particular we employed $r_d = 0$ (model *D0*), $r_d = 0.1\,\sigma_0$ (model *D1*), $r_d = 0.2\,\sigma_0$ (model *D2*). The different bond lengths, representing the difference of length between the five alkyl chains attached to the triphenylene core and the linker, were scanned to study the effect of linker length on the phase behaviour. Regarding the simulation details, first we have equilibrated for 2,000 MC kcycles each of the three dimeric samples at $T^* = 2.2$, and then we have performed production runs of 500 kcycles in order to be able to calculate the observable values we were interested in. Then the next, lower temperature, case was studied, using as starting configuration an equilibrated one resulting from the previous computation at higher temperature, and so on for the remaining temperatures to be investigated.

### 3.1 Simulation results

We have determined from the simulations various useful physical quantities: average of dimensionless internal energies $\langle U^*_{GB} \rangle \equiv \langle U_{GB} \rangle / \epsilon_0$ and $\langle U^*_{BND} \rangle \equiv \langle U_{BND} \rangle / \epsilon_0$, number density $\langle \rho^* \rangle \equiv \langle \sigma_0^3 N / V \rangle$, and orientational order parameter $\langle P_2 \rangle$ reported in Table 1.

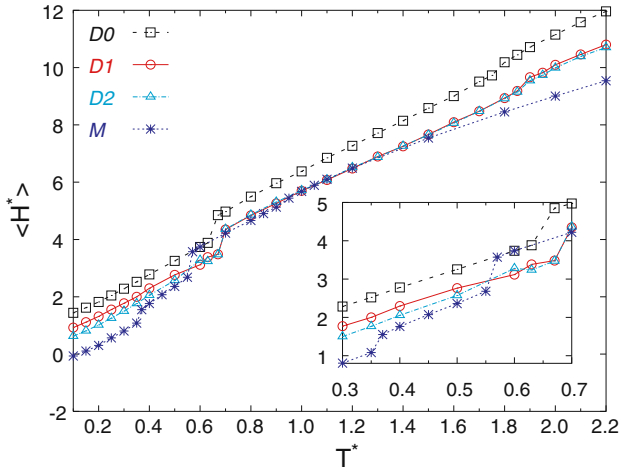


**Fig. 3** Enthalpy $\langle H^* \rangle$ per particle of the three dimeric systems (*D0, D1, D2*), and the monomer (*M*) as a function of the dimensionless temperature $T^*$. In the *inset* a zoom on the region $T^* = 0.3$–$0.7$

Regarding the computed $\langle U^*_{\mathrm{BND}} \rangle$, we see that *D0* differs from both *D1* and *D2*, being definitely higher. As a matter of fact, in the case of the dimer with spacer length equal to zero, the equilibrium distance corresponds to the two monomers touching each other, thus any attempt to increase this distance results in negative values of the GB energy and positive ones of the binding energy to compensate. This effect is not present in the case of the two other dimers where the assumed equilibrium distance falls in the attractive region of the GB monomer–monomer potential.

Here we have performed constant pressure calculations and then we concentrate on the enthalpy $H^* \equiv U^*_{\mathrm{GB}} + U^*_{\mathrm{BND}} + P^*/\rho^*$ (Fig. 3). The enthalpy curve does not present relevant differences in the behaviour between models *D0*, *D1* and *D2*, except for the fact that *D0* displays a jump at lower temperature compared to the other two, i.e., $T^* = 0.63$ instead of $T^* = 0.70$ (see the inset of Fig. 3), indicating a shift of the transition at a slightly lower temperatures. The most notable dissimilarity is between the dimers and the monomer, which, apart from exhibiting a first jump on cooling at a considerably lower temperature than *D0*, also presents two other jumps, a smaller one first, and then a more significant one at a lower temperature ($T^* = 0.35$), which cannot be interpreted considering only the enthalpy. In Fig. 4 we report typical snapshots for three state points inside the different regions. These instantaneous configurations show at once that the phases obtained on cooling correspond to isotropic, nematic and columnar.

In particular, the *D0* model undergoes a jump at $T^* \approx 0.63$, corresponding to the first-order nematic–columnar transition [24], while the *D1* and *D2* model show a transition at $T^* \approx 0.7$. On the other hand, the monomer *M* displays three phase transitions at $T^* = 0.35$, $T^* = 0.55$, and a change in slope at about $T^* = 0.8 - 0.9$. From these data it seems clear that for the dimers the transition occurs at higher temperatures with respect to the monomers. However, it is useful also to examine the orientational order behaviour, certainly more specific for liquid crystalline systems.

Here, we have measured the orientational order of the constituent disc particles, both in the case it refers to a whole molecule as for the monomer, or to one of the two units making the dimer, through the second rank average Legendre polynomial $\langle P_2 \rangle = \langle (3(\hat{\mathbf{z}}_i \cdot \mathbf{Z})^2 - 1)/2 \rangle_i$, where $\hat{\mathbf{z}}_i$ is the disc axis (cf. Fig. 1) and $\mathbf{Z}$ the preferred direction (the director) of the phase.

Examining Fig. 5, it is clear that the behaviour of the systems generally corresponds to the changes of organization already hinted by the jumps in the enthalpy graph discussed above. In addition a steep increase in $\langle P_2 \rangle$ values is visible at about $T^* = 1.9$ for the dimers *D0, D1, D2* and between $T^* = 1.1 - 0.9$ for the monomer *M*, in correspondence of the isotropic–nematic transition, barely visible from the enthalpy plots, because of its very weak first-order character. The dimeric systems exhibit a sharp transition from isotropic to nematic discotic at a much higher temperature than the monomer, which in turn shows a more gradual increase of $\langle P_2 \rangle$, reaching, at $T^* \approx 1.1$ the same type of organization, however, considerably less ordered than that of the dimer. We can conclude that the binding of two monomers creating a dimer favours a higher degree of order in the system with respect to the monomer alone, making it easier to organize the molecules into a more regular system. Regarding the second transition, that is the nematic discotic–columnar one, the only relevant distinction lies in the fact that, as for the previous one, the monomer displays an increase in orientational parameter at lower temperature than *D0, D1, D2* (inset of Fig. 5), but this time, the degree of order reached is roughly the same, with no additional increase of the dimers plots. We notice that the monomer shows another small but distinguishable step at $T^* = 0.35$ that most likely corresponds to the columnar–solid crystalline transition.

Even though the snapshots already shown clearly indicate the molecular organization formed, we should stress that they correspond to istantaneous configurations. A more quantitative information, averaged over all runs, can be obtained from the radial distribution function $g(r) = 1/(4\pi r^2 \rho) \langle \delta(r - r_{ij}) \rangle_{ij}$, which estimates the probability of finding other monomers at a given radius from each monomer composing the system, averaged on all the possible configurations. From the plots in Fig. 6, where for each dimer the contribute from the linked monomer has been subtracted, it is possible to observe a big increase going from $T^* = 2$ to $T^* = 0.25$ in the peak at $r = 0.47\sigma_0$, corresponding to the face-to-face stacking, which indicates an increase in the degree of structuring along the columnar axis. The enhancement of this peak goes together with the appearance of two other smaller ones at distances equal to multiples of $0.47\,\sigma_0$, corresponding to the second and

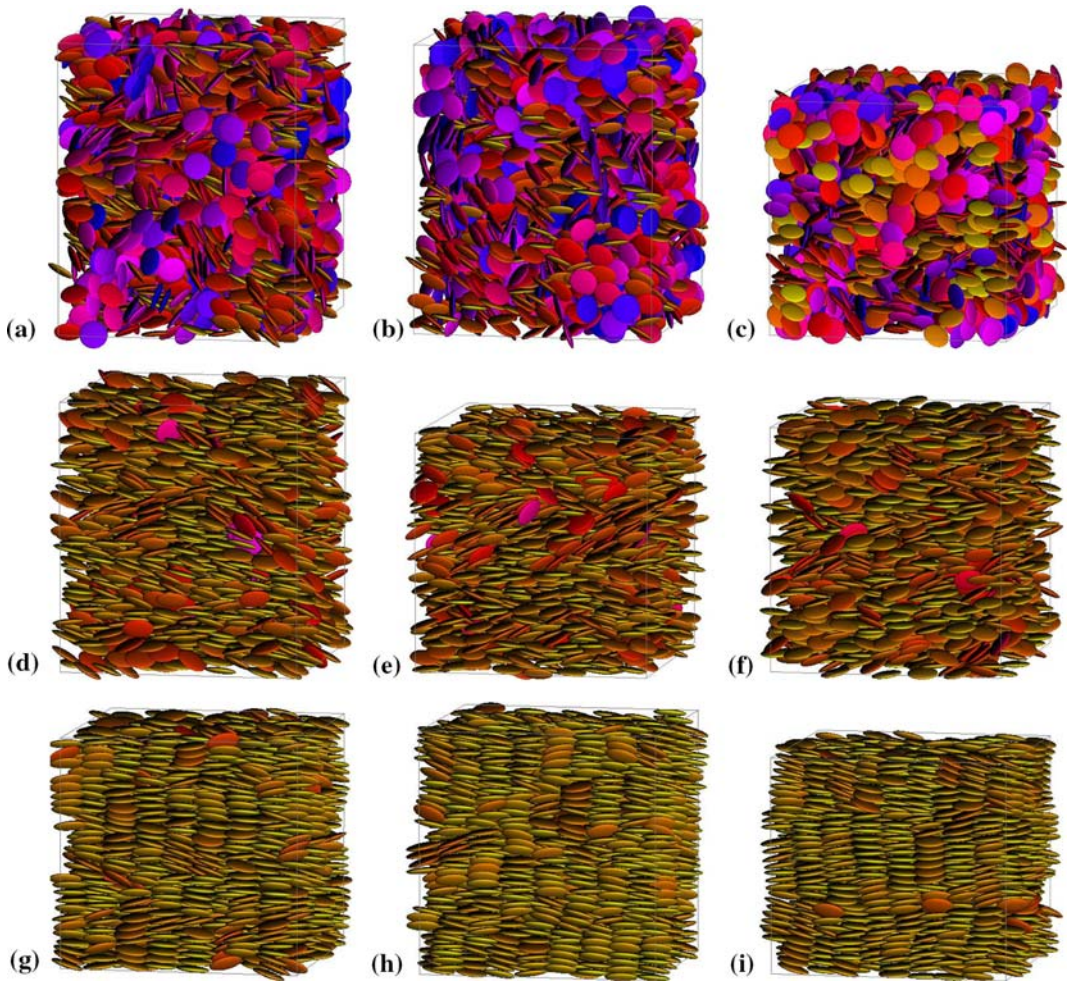


**Fig. 4** Snapshots at $T^* = 2.0$ (**a–c**, isotropic), 1.0 (**d–f**, nematic discotic), 0.25 (**g–i**, hexagonal columnar). From *left* to *right*: *D0*, *D1*, *D2*. The orientation of the molecules, with respect to the director, is rendered using a color coding ranging from *yellow* (parallel) to *blue* (perpendicular)

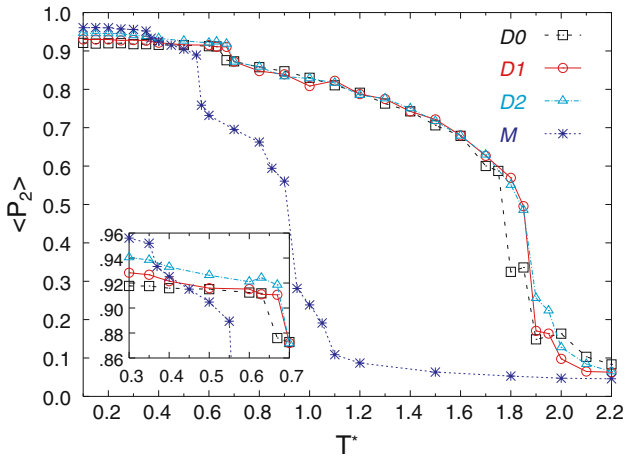


**Fig. 5** Average orientational parameter of a disc $\langle P_2 \rangle$ for the three dimeric systems (*D0, D1, D2*) and the monomer *M* as a function of the dimensionless temperature $T^*$. In the inset a zoom on the region $T^* = 0.3 - 0.7$

third neighbours along the column. All the $g(r)$ plots show another characteristic peak at $r \approx 1.9\ \sigma_0$, which corresponds to the monomer side-to-side interactions between two different dimers, and, for the plots of the sample in the columnar phase, Figs. 6c, d also reveal a possible degree of regularity between the columns, that assemble themselves generating a "supraorganization", such as the hexagonal columnar $Col_h$ structure reported by most of the researchers dealing experimentally with discotic systems [1–5,10,25–29].

We now go back to the observation, already made, of the lack of crystallization for the dimers, that could be connected to the formation of glassy systems. To test this, we have calculated and we report in Fig. 7 the values of the average mean square displacement after 25 MC kcycles $\langle \Delta r^2 \rangle$ for the discs as a function of temperature as an indicator of mobility.

From Fig. 7 it is once more apparent that the monomer *M* behaves differently from all the three dimers *D0, D1, D2*: while the dimers displacements decrease abruptly around

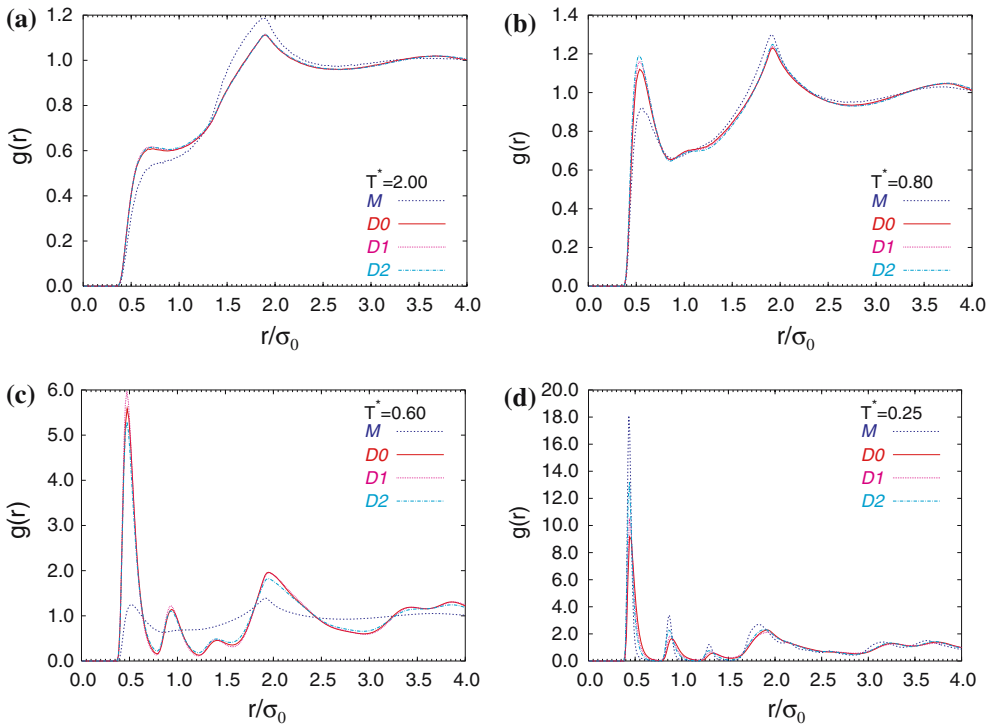


**Fig. 6** Radial distribution functions $g(r)$ for the three dimeric systems (*D0, D1, D2*) and the monomer *M*, measured at $T^* = 2.0$ **(a)**, 0.8 **(b)**, 0.6 **(c)**, 0.25 **(d)**

$T^* = 0.65 - 0.7$, in coincidence with the nematic–columnar transition, the monomer curve displays a marked drop at about $T^* = 0.55$, still indicating not only the same kind of transition, but also another one around $T^* = 0.35$, probably representing a columnar to solid transition. Moreover, the value of mobility reached by *M* at this first change of slope is at least three times higher than those pertaining to *D0, D1, D2* at higher temperature at which they convert from nematic to columnar; the latter value on the other hand is more or less equal to the mobility typical of *M* at the lowest temperature transition ($T^* = 0.35$).

This indicator thus leads us to a more detailed interpretation of the different structures our systems organize into: first *M* turns from nematic to columnar hexagonal phase, characterized by a certain freedom of movement of the particles, then the system freezes into a solid state in which the particles change their organization, by interdigitating one another. On the contrary, the dimers mobility greatly reduces already at the nematic to columnar transition, with similar features to the experimental results given by Kranig et al. [23]: oligomers made up of two units, when cooled down to lower temperatures, result in highly ordered anisotropic glasses. In fact, the resulting columns are interlinked and form networks, thus limiting the particle diffusion. These interconnections can be clearly seen in the snapshots shown in Fig. 8: it is the single discs forming the dimers that line up constituting the columns, but one cannot distinguish any long-range regular

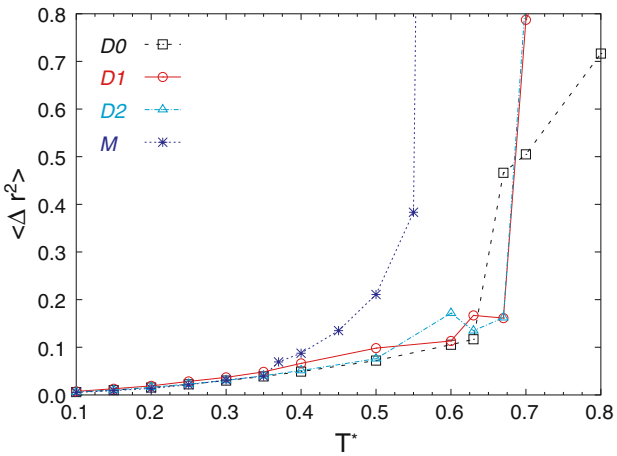


**Fig. 7** Total mean square displacement $\langle \Delta r^2 \rangle$ plots ($\sigma_0^2$ units) at the various temperatures $T^*$ simulated for the three dimeric systems *D0, D1, D2* and the monomer *M*, calculated after 25 MC kcycles

piling up of the linkers joining the two monomers together. This interconnected network confers significant rigidity to the system, making it more similar to a polymeric system, rather than to a monomeric one.

## 4 Conclusions

We have studied the physical properties of the simplest liquid crystalline discotic dimer, composed by two identical moie-

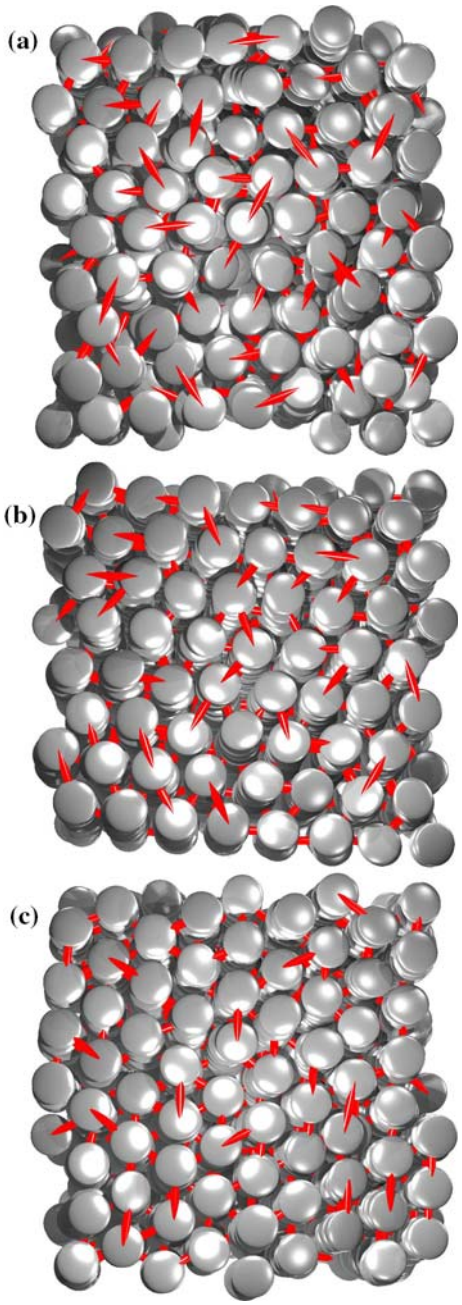


**Fig. 8** *Top views* of instantaneous configurations in the columnar phase ($T^* = 0.25$): system *D0* **(a)**, *D1* **(b)**, *D2* **(c)**. The *red cylinders* represent the bonds connecting two monomers

ties attached via a flexible linker and compared with the ones of the constituting monomer, by MC simulations. In agreement with experimental evidence [10], this study underlines that dimerization produces dramatic changes in the transition temperatures and in the phase behaviour. In particular, with respect to the monomer, we found an increase in the clearing temperature and the columnar–nematic transition temperature, a broadening of the nematic phase range and an enhancement of the order. We have also found a suppression of the crystalline phase in favour of a wider columnar phase, formed by columns of stacked monomers and characterized by low translational diffusion.

The investigation of the effect of the spacer length lead to the observation that very short spacers (*D0*) limit the dimer capability of assembling in columns, with an attendant reduction of the columnar phase range and of the degree of the orientational order.

We believe that the present GB model dimers represent a good starting model also for the study of phase organization of more complex discotic polymeric structures at coarse grained level and we plan to extend the study in this direction, e.g. to investigate the conditions for the formation of lamellar or columnar phases, until now still poorly understood.

**Acknowledgments** We gratefully acknowledge MIUR and the European Union for supporting this study through the project PRIN "Modelling and characterisation of liquid crystals for nano-organised structures" and the EU Integrated Project NAIMO (No.NMP4-CT-2004-500355).

## References

1. Wan W, Monobe H, Tanaka Y, Shimizu Y (2003) Liq Cryst 30:571
2. Kumar S (2006) Chem Soc Rev 35:83
3. Kumar S (2004) Liq Cryst 31:1037
4. Brunsveld L, Folmer BJB, Meijer EW (2000) MRS Bull 25:49
5. Bushby RJ, Lozman OR (2002) Curr Opin Colloid Interface Sci 7:343
6. Muccioli L, Berardi R, Orlandi S, Ricci M, Zannoni C (2006) Theor Chem Acc. DOI: 10.1007/s(X)214-006-0229-7
7. Lemaur V, da Silva Filho DA, Coropceanu V, Lehmann M, Geerts Y, Piris J, Debije MG, van de Craats AM, Senthilkumar K, Siebbeles LDA, Warman JM, Brédas JL, Cornil J (2004) J Am Chem Soc 126:3271
8. Perova TS, Jagdish KV (2004) Adv Mater 7:919
9. Kumar S (2003) Pramana J Phys 61:199
10. Kumar S (2005) Liq Cryst 32:1089
11. Grother SCM, Sear RP, Jackson G (1997) J Chem Phys 106:7315
12. Luckhurst GR, Romano S (2003) Phys Chem Chem Phys 5:1242
13. Luckhurst GR, Romano S (2005) Phys Chem Chem Phys 7:2821
14. Berardi R, Fehervari M, Zannoni C (1999) Mol Phys 97:1173
15. Berardi R, Micheletti D, Muccioli L, Ricci M, Zannoni C (2004) J Chem Phys 121:9123
16. Micheletti D, Muccioli L, Berardi R, Ricci M, Zannoni C (2005) J Chem Phys 123:224705
17. Zannoni C (2001) J Mater Chem 11:2637
18. Berardi R, Emerson APJ, Zannoni C (1993) J Chem Soc Faraday Trans 89:4069
19. Emerson APJ, Luckhurst GR, Whatling SG (1994) Mol Phys 82:113
20. Berardi R, Orlandi S, Zannoni C (2005) Liq Cryst 32:1427
21. Caprion D, Bellier-Castella L, Ryckaert JP (2003) Phys Rev E 67:041703
22. Orlandi S, Muccioli L, Ricci M, Berardi R, Zannoni C (2007) (to appear)
23. Kranig W, Huser B, Spiess HW, Kreuder W, Ringsdorf H, Zimmermann H (1990) Adv Mater 2:36
24. Kouwer PHJ, Jager WF, Mijs WJ, Picken SJ (2000) Macromolecules 33:4336

25. Feng X, Pan C (2002) Chem Phys Chem 6:539
26. Boden N, Bushby R, Lu Z (1998) Liq Cryst 25:47
27. Disch S, Finkelmann H, Ringsdorf H, Schuhmacher P (1995) Macromolecules 28:2424
28. Boden N, Bushby RJ, Cammidge AN (1995) J Am Chem Soc 117:924
29. Zhang W, Horoszewski D, Decatur J, Nuckolis C (2003) J Am Chem Soc 125:4870